Development of an inhalable antiviral powder formulation against respiratory syncytial virus

Heida, Rick; Akkerman, Renate; Silva, Paulo H. Jacob; Lakerveld, Anke; Ortiz, Daniel; Bigogno, Chiara; Gasbarri, Matteo; Van Kasteren, Puck B.; Stellacci, Francesco; Frijlink, H.W.

Published in:
Journal of Controlled Release

DOI:
10.1016/j.jconrel.2023.03.059

Publication date:
2023

Journal of Controlled Release 357 (2023) 264–273

Contents lists available at ScienceDirect

Journal of Controlled Release

journal homepage: www.elsevier.com/locate/jconrel

Development of an inhalable antiviral powder formulation against respiratory syncytial virus

Rick Heida [a], Renate Akkerman [a,b], Paulo H. Jacob Silva [c], Anke J. Lakerveld [d], Daniel Ortiz [e], Chiara Bigogno [f], Matteo Gasbarri [c], Puck B. van Kasteren [d], Francesco Stellacci [c], Henderik W. Frijlink [a], Anke L.W. Huckriede [b], Wouter L.J. Hinrichs [a,*]

[a] Department of Pharmaceutical Technology and Biopharmacy, University of Groningen, 9713 AV Groningen, the Netherlands
[b] Department of Medical Microbiology and Infection Prevention, University of Groningen, University Medical Center Groningen, 9713 AV Groningen, the Netherlands
[c] Institute of Materials, Ecole Polytechnique Fédérale de Lausanne (EPFL), Lausanne 1015, Switzerland
[d] Centre for Infectious Disease Control, National Institute for Public Health and the Environment (RIVM), 3720 BA Bilthoven, the Netherlands
[e] Institute of Chemical Sciences and Engineering, Ecole Polytechnique Fédérale de Lausanne (EPFL), Lausanne 1015, Switzerland
[f] Aphad Srl, Buccinasco 20090, Italy

ARTICLE INFO

Keywords:
Entry inhibitor
Broad-spectrum
Spray drying
Dry powder inhalation
Pulmonary drug delivery
Respiratory syncytial virus

ABSTRACT

Respiratory viruses including the respiratory syncytial virus (RSV) aggravate the global burden of virus-inflicted morbidity and mortality. Entry inhibitors are a promising class of antiviral drugs for combating these viruses, as they can prevent infection at the site of viral entry, i.e., the respiratory tract. Here we used a broad-spectrum entry inhibitor, composed of a β-cyclodextrin backbone, functionalized with 11-mercapto-1-undecanesulfonate (CD-MUS) that is capable of neutralizing a variety of viruses that employ heparan sulfate proteoglycans (HSPG) to infect host cells. CD-MUS inactivates viral particles irreversibly by binding to viral attachment proteins through a multivalent binding mechanism. In the present study, we show that CD-MUS is well tolerated when administered to the respiratory tract of mice. Based on this, we developed an inhalable spray-dried powder formulation that fits the size requirements for lung deposition and disperses well upon use with the Cyclops dry powder inhaler (DPI). Using an in vitro dose-response assay, we show that the compound retained its activity against RSV after the spray drying process. Our study sets the stage for further in vivo studies, exploring the efficacy of pulmonary administered CD-MUS in animal models of RSV infection.

1. Introduction

Throughout history, there has been a continuous emergence of respiratory viruses with epidemic and pandemic potential, including influenza A virus, respiratory syncytial virus (RSV) and, recently, SARS-CoV-2 [1]. Respiratory viruses heavily contribute to the global burden of virus-inflicted morbidity and mortality and thus, the urgency for effective prevention and treatment options remains high [2,3]. RSV infections mainly form a risk for infants [4,5] and the elderly [6]. Recently, a rise in RSV cases has been observed after measures for the prevention of SARS-CoV-2 transmission were gradually lifted. This has led to an increased cumulative pressure on healthcare and an increased chance of severe coinfections [7,8]. Up to this date, no effective vaccine is available, although many candidates are in development [9]. The standard of care treatment has largely been supportive (e.g. through mechanical ventilation) or has been based on the occasional use of the nebulized nucleoside analog ribavirin [10]. In high-risk infants, immune-prophylaxis is performed by using repeated injections of the monoclonal antibody palivizumab [11]. Recently, an improved single-dose monoclonal antibody, nirsevimab, has been granted market authorization in Europe for the prophylaxis against RSV infection in new-born infants [12]. Nevertheless, both limited efficacy and laborious treatment procedures push the development of novel drugs [10,13,14].

Entry inhibitors are a promising class of antiviral drugs as they can prevent a virus from entering the cell and thereby tackle the earliest step in the viral infection process [15]. However, previous entry inhibitors either lacked efficacy owing to their reversible, i.e. virustatic mechanism of action, or led to cellular toxicity [16]. Earlier work from the Lausanne group has reported a novel class of entry inhibitors based on gold nanoparticles functionalized with long flexible linkers that terminate in

* Corresponding author.
E-mail address: w.l.j.hinrichs@rug.nl (W.L.J. Hinrichs).

https://doi.org/10.1016/j.jconrel.2023.03.059
Received 15 February 2023; Received in revised form 28 March 2023; Accepted 31 March 2023

11-mercapto-1-undecanesulfonate (MUS) groups [17]. These compounds were designed to mimic heparan sulfate proteoglycans (HSPGs), that function as an attachment factor for many viruses and are localized on the eukaryotic cell membrane [18]. Based on a multivalent binding mechanism, the compounds were designed to irreversibly disrupt the membrane of HSPG-targeting viruses, thus exerting a virucidal effect [17]. Because the drug mimics a common component of viral attachment, the molecules showed broad-spectrum activity. The efficacy of the MUS-functionalized gold nanoparticles has been confirmed against several distinct HSPG-targeting viruses, both in vitro and in vivo. Specifically, the nanoparticles were able to inhibit respiratory syncytial virus (RSV) infection in mice without any signs of toxicity [17]. More recently, these MUS-carrying gold nanoparticles have been successfully replaced by a biocompatible and commonly used β-cyclodextrin core (CD). Both in vitro and ex vivo studies have shown that these MUS-carrying cyclodextrins (CD-MUS) are virucidal against a variety of viruses, including RSV, and no adverse effects have been detected so far [19,20].

When used against respiratory pathogens like RSV, entry inhibitors should preferably be delivered to the respiratory tract. Since the pathogenesis of a severe RSV infection involves progression to the lungs, the drug should ideally be targeted to the lower respiratory tract to ensure optimal bio-availability [21]. From this perspective, administration of CD-MUS by inhalation could be advantageous. Considering the limited stability of liquid formulations and challenges regarding their administration, it would be beneficial to formulate these compounds into a dry form, as they can easily be administered using a dry powder inhaler (DPI). Dry powder formulations for inhalation have been used to target other diseases, e.g. bacterial infections and chronic airway diseases, but have not yet been extensively explored for antiviral therapy.

Therefore, in the present study, we first assessed the pharmacokinetic properties of CD-MUS after administration of the compound to the respiratory tract of mice. Subsequently, we developed a dry powder formulation of CD-MUS for inhalation to target RSV in the lower airways. To this end, we used spray drying to prepare a powder that meets the physical requirements for lung deposition based on its geometric and aerodynamic properties, and that performs well in a DPI. Using an in vitro dose-response assay against two strains of RSV, we confirmed that the compound retained its activity after drying. The work presented here could aid further development of the compound as inhalable product and sets the stage for in vivo RSV infection studies, comparing the efficacy and safety of pulmonary administered CD-MUS with other routes of administration.

2. Materials and methods

2.1. CD-MUS synthesis and characterization

To synthetize CD-MUS (Fig. 1), a modification of the synthetic route reported by Jones et al. was used [19]. In short, heptakis-(6-deoxy-6-mercapto)-β-CD (3 g, 2.4 mmol, Arachem, Kuala Lumpur, Malaysia) and sodium undec-10-ene-1-sulfonate (8.6 g, 33.6 mmol), were suspended in 200 mL of MilliQ water in a 500 mL round bottom flask. The reaction mixture was stirred using magnetic stirring (600 rpm) and placed in front of a 400 W ultraviolet (UV) lamp for 12 h. The turbid mixture became clear after this interval and the entire crude was placed inside 2 kDa dialysis membranes (45 mm wide, Spectra/Por®, Spectrum Laboratories Products Inc., New Brunswick, NJ) and dialysed for 4 consecutive days against 2 L of MilliQ water that was replaced four times a day. After the four days of dialysis, the content inside the dialysis membranes was filtered through a 0.2 μm syringe into eight 45 mL Falcon Tubes (total volume > 200 mL) frozen and lyophilised. By this means, 6.2 g of slightly off-white powder was collected (85% yield). To characterize the sample, high resolution mass spectrometry (HRMS) analyses were performed as described previously [18]. A brief description can be found in the supplementary material (Supplementary method 1).

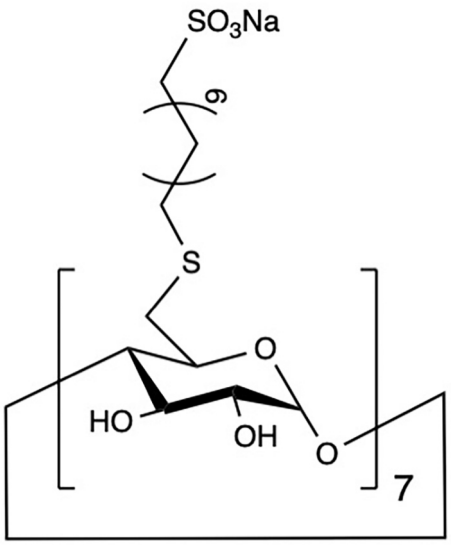

Fig. 1. Chemical structure of CD-MUS. The counterion to each sulfonate group is a sodium.

2.2. In vivo pharmacokinetics study

2.2.1. Animal study protocol

Envisioning a possible use for pulmonary administered CD-MUS as a therapeutic agent against RSV, a study was performed in collaboration with Aphad analytical solutions (Buccinasco, Italy). The aims were to establish general pharmacokinetic properties and organ distribution of the compound when administered intranasally as an aqueous solution to mice. The in vivo study was conducted by Farefarma-Emozoo (Casole d'Elsa, Siena, Italy) and adhered to the Italian Ministry of Health guidelines for the use and care of experimental animals (authorization 173/2018-PR phase B D4A18.B.G7M). For this study, a total of 28 male Swiss CD1 mice with an average body weight of 33 ± 1 g were obtained from Envigo (Udine, Italy). Mice were 5 weeks old upon arrival and were housed under standard conditions (12-h light/dark cycle) with free access to food and water. After a 5-day acclimatization period, mice were divided randomly in groups of 4. Preceding treatment, mice were sedated using mild isoflurane anesthesia (2.5%). The animals received a 9 mg/kg dose of CD-MUS in H_2O via intranasal instillation (15 μL per mouse, divided over each nostril). Based on previous work, it can be assumed that in anesthetized animals, such a volume progresses down to the lungs, ensuring delivery to the whole respiratory tract [22]. Each group was then euthanized at a given time-point (i.e. 15 min, 30 min, 1, 2, 4, 6, and 24 h post-administration) after which different organs (lung, liver, kidney, pancreas, spleen and brain) and blood were collected. The organs were washed in saline, dried on paper and weighted immediately after collection. Organs were then frozen at −80 °C until further analysis. Blood was retrieved via exsanguination of the caudal vein up to a volume of 200–300 μL and centrifuged at 3000 rpm for 10 min at 4 °C for plasma collection.

2.2.2. Determining tissue and plasma concentrations of CD-MUS after administration using liquid chromatography with tandem mass spectrometry

50 μL of plasma was mixed with 5 μL of Internal Standard (200 ng/mL of Pyridyl diphenyl triazine disulfonic acid sodium salt in water, Sigma-Aldrich, St Luis, MO, USA) and with 200 μL of cold (4 °C) MeOH. After mixing for 10 min at 300 rpm, samples were centrifuged for 15 min at 4600 rpm (5 °C). Subsequently, the supernatant was transferred to a 96-well plate (Phenomenex, Torrance, CA, USA) and dried with a ScanSpeed MiniVac (Labogene, Lillerød, Denmark), resuspended in 150 μL of water and injected into the LC-MS/MS. Organs were weighted either after the sacrifice or before analysis (in case of the pancreas) and

homogenized in 20 mM ammonium formate (0.2 g/mL) with a Precellys 24 homogenizer (Bertin technologies, Montigny-le-Bretonneux, France) using Precellys Lysing CK28 beads, except for the pancreas for which CK14 beads were used. Solid Phase Extraction (SPE) was then performed using a Strata-X-AW 33 μm Polymeric Weak Anion (30 mg/well in a 96-well plate (Phenomenex)). Preceding the extraction, the SPE plate was washed with 1 mL of methanol and conditioned with 1 mL of water. 50 μL of tissue homogenate was mixed with 5 μL of internal standard and diluted in 450 μL of water. Samples were then vortexed thoroughly for 1 min and centrifuged. Supernatants were loaded on the SPE plate that was then washed with 0.5 mL of 20 mM ammonium formate (pH 6.6) followed by 0.5 mL of methanol. CD-MUS was eluted with 250 μL of 5% NH_4OH in MeOH for 3 times. The 3 fractions were then pooled together, dried and resuspended in 200 μL of 5 mM Ammonium Bicarbonate in water (pH 8) and MeOH (75:25 ratio). Samples were then sonicated for 10 min, shaken for 10 min at 500 rpm and centrifuged at 4600 rpm for 15 min. Samples were then analyzed after purification by liquid chromatography with tandem mass spectrometry (LC-MS/MS) using a HPLC (Shimadzu, Kyoto, Japan) coupled with the API 4500QTrap (AB Sciex LLC, Framingham, MA, USA). The mobile phases were 5 mM Ammonium Bicarbonate in water (A, pH 8) and MeOH (B) with a 0.3 mL/min flow and a linear gradient from 0.5% B to 95% in 1.5 min followed by an isocratic step at 95% B up to 4.5 min. The column used was a Kinetex (Phenomenex) 2.6 μm C18 100A 75*3 mm. Samples were acquired in negative mode using multiple reaction monitoring (MRM). 576.4 $[M\text{-}5H]^{5-}$ and 480.2 $[M\text{-}6H]^{6}$ were selected as parent Ions for the MRM with the transitions reported in Supplementary Table 1. Interface parameters were: Gas 1:50; Gas 2:45; collision activated dissociation (CAD): High; curtain gas (CUR): 30; source temperature: 500 °C; IS -4500; Entrance Potential (EP): −10 V; dwell time: 100 msec.

2.3. Powder formulation

CD-MUS powders were produced by spray drying. To aid deagglomeration of the spray-dried powder formulation, 4% *w*/w trileucine (relative to the total solute content, Bachem AG, Bubendorf, Switzerland) was included to obtain low cohesiveness of the resulting powder particles [23–25]. Feed solutions at a total solute concentration of 2% *w/v* in Milli-Q water (20 mg/mL) were spray dried using a Büchi Mini Spray Dryer B-290 in conjunction with a B-296 dehumidifier (both from Büchi AG, Flawil, Switzerland). The drying procedure was performed at a feed rate of 3 mL/min using an NE-300 syringe pump (ProSense B.V., Oosterhout, The Netherlands) with a 60 mL syringe (Codan B.V., Deventer, The Netherlands). Preceding drying, the syringe was connected via a small rubber tubing to the feed port of a two-fluid nozzle (1.5 mm cap). Samples were fed into the system at an atomizing gas flow of 601 $L_N\ h^{-1}$ (rotameter set to 50 mm). The inlet temperature was set to 120 °C and the aspirator was set to 100%, which, according to the operation manual corresponds to an aspiration flow of approximately 35 $m^3\ h^{-1}$ at maximum. This resulted in an outlet temperature during drying of 58 °C. To determine the yield, the glass collection vial was weighed before and after the drying procedure. The powder was then sealed and stored under 0% relative humidity to prevent potential moisture uptake until further analysis. As a mock treatment for the dose-response experiments described below, we spray-dried ß-cyclodextrin (Royal Avebe U.A., Foxhol, The Netherlands), also formulated with 4% *w*/w trileucine (Bachem AG). In order to ensure that CD-MUS retained its molecular integrity after drying, the compound was again analyzed with HRMS as described in section 2.1.

2.4. Powder characterization

2.4.1. Powder morphology and primary particle size analysis

In order to assess the morphology of the spray-dried particles, scanning electron microscopy (SEM) was performed, using a JSM 6460 SEM (JEOL, Tokyo, Japan) as described previously [26]. To determine the primary particle size of the spray dried powder, laser diffraction analysis was performed using the RODOS disperser at 3 bar in conjunction with a HELOS BF diffraction unit (both from Sympatec GmbH, Clausthal-Zellerfeld, Germany). The diffractor was equipped with an R3 lens (100 mm) allowing detection of particles within a range of 0.1 to 175 μm. Before each measurement, a reference measurement was performed for 5 s. Approximately 50 mg of powder was then carefully loaded on the rotating disk using a spatula. Measurements were triggered when an optical density of 0.2% was reached on channel 30 and were stopped after 3 s. The particle size distribution was computed based on the Fraunhofer diffraction theory, from which the X10, X50 and X90 values were derived. These values correspond to the cumulative volume percent values (10%, 50% and 90%, respectively) of the resulting particle size distribution curve. In addition, the span, or distribution width, was calculated using the below equation in order to assess powder homogeneity.

$$Span = \frac{(X90 - X10)}{X50}$$

2.4.2. Dispersion efficiency

Powder dispersibility was assessed using the Cyclops™ DPI [27] (PureIMS, Roden, The Netherlands). The particle size distribution of the emitted aerosol was determined by laser diffraction analysis using a HELOS BF diffraction unit equipped with the Inhaler2000 adapter (Sympatec GmbH) and a custom-made mouthpiece. Before each measurement, a reference measurement was performed to control for minor differences in the resistance of different cyclops inhalers. For each measurement, either 50 or 30 mg of powder was loaded in the device, with or without 10 mg of α-lactose monohydrate crystals (250–315 μm, derived from Pharmatose® 80 M, DFE Pharma, Goch, Germany). Because of their size, these crystals do not leave the inhaler but rather function as a sweeper to prevent adhesion of powder particles to the wall of the cyclops classifier and therefore, to minimize the inhaler retention [27]. An R3 lens (100 mm) was used enabling a measuring range between 0.1 and 175 μm. All measurements were performed at a pressure drop of 4 kPa (40 mbar). Measurements were triggered when the measured optical density passed 0.2% and lasted 3 s. Based on the data, the fine particle fraction (FPF), defined as the percentage of particles $\leq$5 μm was determined. The FPF is generally considered a measure for the fraction of particles that reach the lungs upon a normal inhalation maneuver. Furthermore, the FPF is a suitable measure for the dispersion efficiency of the formulation and inhaler combination used.

2.5. Cascade impaction analysis

2.5.1. Assessing the aerodynamic behavior using the next generation impactor

To determine the aerodynamic particle size distribution after dispersion of the dried CD-MUS formulation from the cyclops inhaler, cascade impaction analysis was performed using a next generation impactor™ (NGI, MSP corp., Shoreview, MN, USA) according to the recommendations for apparatus E in chapter 2.9.18 of the *European Pharmacopoeia* [28]. In short, the NGI is equipped with a standard USP/Ph. Eur. induction port that models the throat, seven stages for the collection of powder particles of different size ranges and a micro-orifice collector (MOC) for catching the finest particles. Before weighing the powders, 10 mg of sweeper crystals were added, as described in section 2.4.2. In order to reduce bounce effects of the high-dose formulation [29], 0.2 μm/50 mm Whatman glass-fiber filters (Cytiva, Marlbourough, MA, USA) were added to all of the impactor stages, with the exception of the MOC, and pre-wetted subsequently with 1 mL of Millipore H_2O. A wash bottle was included downstream of the NGI to catch any remaining ultra-fine particles. The inhaler with powder was connected to the NGI via a custom-made, airtight mouthpiece. The measurements were performed for 3 s at a pressure drop of 4 kPa, to match the laser diffraction

measurements. This corresponded to a flowrate through the NGI of 52.8 L*min^{-1}. After measuring, all impactor stages, the induction port and micro-orifice collector were rinsed 3 times with one 30-minute interval and two 15-minute intervals to ensure complete dissolution of the powder. Hereafter, the samples were collected in pre-weighed collection cups and the filters were discarded. After collection, all cups were weighed again to calculate the sample volume.

2.5.2. Sample analysis

Preceding analysis of the collected powder fractions, the samples retained from stage 1 to 7 were filtered with Phenex 26 mm/0.2 µm RC filters (Phenomenex) to remove any remaining glass fibers. Hereafter, the dose per collection cup was analyzed by using the colorimetric anthrone reaction for carbohydrates in solution [30]. In short, 4 mL of a 2 mg/mL solution of anthrone (Sigma-Aldrich) in concentrated analytical grade sulfuric acid (Boom B.V., Meppel, The Netherlands) was carefully added to 1 mL of sample and to 1 mL of prepared calibration samples (containing the same spray-dried batch of CD-MUS with trileucine) at a known concentration range of 0–500 µg/mL. After brief vortexing, the samples were left to incubate for 10 min. 250 µL was then transferred on a 96-wells plate together with the standard. Subsequently, the absorbance was read at a wavelength of 620 nm using a Synergy HT plate reader (BIO-TEK Instruments Inc., Winooski, VT, USA). Based on the values of the calibration curve, the amount of powder per collection cup was calculated after subtraction of the blank (0 µg/mL). Next, the stage-specific cut-off diameters were calculated based on recommendations of the *European Pharmacopoeia* for apparatus E in conjunction with the procedure for powder inhalers [28]. Subsequently, the relative deposition across the stages, as well as the FPF and the mass median aerodynamic diameter (MMAD) were derived using non-linear curve-fitting as described before [31].

2.6. In vitro efficacy of dry-powder formulated CD-MUS against RSV

2.6.1. Cell line and viruses

To investigate whether the CD-MUS retained its activity upon drying, a dose-response assay was performed on Vero-cells. To this end, Vero-cells (ATCC CCL-81) were cultured in Dulbecco's Modified Eagle Medium (DMEM; Gibco, Life Technologies, Carlsbad, CA, USA) supplemented with 5% heat-inactivated fetal bovine serum (HyClone, Thermo Fisher Scientific, Waltham, MA, USA) and 1% penicillin, streptomycin, and glutamine (PSG, Gibco). Human recombinant RSV-X-GFP (based on clinical isolate 98–25147-X and described in [32]), further referred to as RSV-A, and human RSV-B (ATCC VR-1400) were propagated in Vero-cells. Virus stocks were purified between layers of 10% and 50% sucrose using an Optima XE-90 Ultracentrifuge (Beckman Coulter, Brea, CA, USA). Samples were centrifuged at a speed of 100,000 x g for 90 min at 4 °C. The 50% tissue culture infective dose ($TCID_{50}$) per mL was determined on Vero cells using the Spearman and Karber method [33].

2.6.2. Dose-response assays

Vero-cells were pre-plated on 24-well plates at a density of 75,000 cells/well and cultured overnight (37 °C, 5% CO_2). Powders were dissolved in sterile water at a starting concentration of 1 mg/mL CD-MUS. Next, 1:5 serial dilutions ranging from 500 to 0.16 µg/mL were made in cell culture medium. As a negative control, spray-dried β-cyclodextrin co-formulated with 4% trileucine was used and diluted in the same way. Subsequently, RSV-A (multiplicity of infection (MOI): 1) or RSV-B (MOI: 0.8) was added to the diluted compounds and incubated for 1 h at 37 °C, 5% CO_2. Hereafter, the virus/compound mixtures were added to the cells and incubated again under the same conditions. Following virus adsorption, the virus inoculum was removed, cells were washed and fresh medium was added to the wells. After 24 h of incubation at 37 °C, 5% CO_2, the percentage of infected cells was analyzed using flow cytometry. For RSV-A, cells were trypsinized and stained with a 1:5000 dilution of Fixable Viability Dye eFluor™ 780 (eBioscience, Thermo Fisher Scientific) for 30 min at 4 °C. In the case of RSV-B, cells were stained with the viability dye in combination with a 1:1000 dilution of anti-human RSV G-FITC (clone 131-2G, Sigma-Aldrich, St. Louis, MO, USA), also for 30 min at 4 °C. Subsequently, cells were fixed using 4% formaldehyde (VWR Chemicals, Radnor, PA, USA) for 15 min at room temperature. Flow cytometry was carried out using the BD FACSCanto™ II flow cytometer (BD Biosciences, Franklin Lakes, NJ, USA). Data were analyzed using FlowJo software (BD Biosciences) and Graphpad Prism version 8.0.1. (GraphPad Software, San Diego, CA, USA). Dose-response curves were made by plotting a non-linear fit curve of the log concentration against the percentage of infection (relative to the untreated control). The flow cytometry gating strategy is shown in Supplementary Fig. 1.

3. Results

3.1. Pharmacokinetics and safety in mice

Before formulating CD-MUS into an inhalable powder, the pharmacokinetics of the compound were determined after intranasal instillation in mice. Mice did not show any deviations in physical appearance and behavior. Also, no anomalies were observed at the dissection of the organs. Fig. 2 shows the pharmacokinetic profiles of CD-MUS in the plasma and in the organs. Immediately after administration, the plasma, pancreas and lungs retained the highest concentration of the compound, confirming that it reached the lungs after intranasal instillation. CD-MUS concentrations in the pancreas and lungs reached the lower limit of detection after 2 and 6 h, respectively. The concentration of CD-MUS in the plasma, however, peaked 4 h post-administration and was still quantifiable up to 24 h. CD-MUS was not detected in the brain and was found only in very small amounts in the liver (detectable only at 15 min, not shown in graph). CD-MUS was also found at low concentrations in the spleen and at higher concentrations in the pancreas where some variability was present, possibly due to the difficulty to excise this organ from the fat tissue. CD-MUS was present from 2 h onwards in the kidney, suggesting renal excretion. CD-MUS concentrations in plasma and tissues are shown in Supplementary Tables 2 and 3, respectively. Additional pharmacokinetic parameters such as the maximum concentration, the half-life of the compound in separate tissues and the mean residence time are shown in Supplementary Table 4. Missing data points indicate values below the limit of quantification.

3.2. Powder characterization

3.2.1. Powder morphology and molecular integrity

After assessment of pharmacokinetic properties, CD-MUS was formulated into a powder using spray drying. SEM images show that

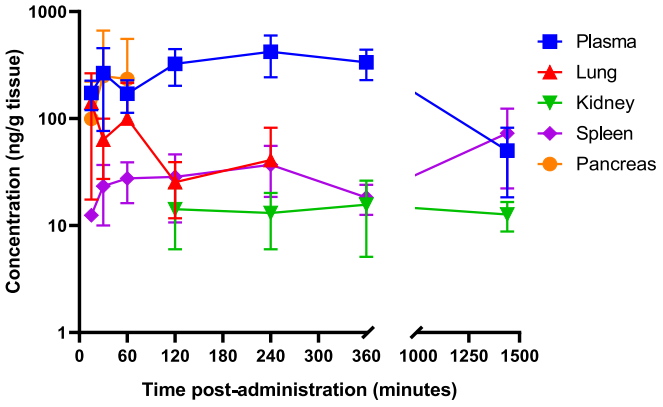

Fig. 2. Mean concentrations of CD-MUS over time in plasma and tissues after intranasal administration. Error bars represent the standard deviation. n = 4 per time point.

most particles exhibit a spherical structure with occasionally a wrinkled surface (Fig. 3). It can be seen that the majority of the single particles are below 5 μm in size. Furthermore, it can be seen that the particles form clusters of particles that vary in size (Fig. 3a). After synthesis, the HRMS spectra, before and after processing the compound into a powder, showed about 90% majority of 7-substituted beta cyclodextrins and species with 6-substituted beta cyclodextrins as the main side product of the reaction, along with traces of 5-substituted forms (Supplementary Fig. 2 and Supplementary Tables 5 and 6). The figures confirm that the molecular integrity of CD-MUS was not deteriorated by the spray drying process.

3.2.2. Particle size distribution and dispersion behavior from the Cyclops DPI

The primary particle size distribution after dispersion by the RODOS device is depicted in Fig. 4a. Upon dispersion, the majority of the spray-dried particles was found to be smaller than 5 μm in diameter, with the fraction ≤5 μm approaching 96%, and an average span of 1.75 μm. After dispersion from the cyclops inhaler (Fig. 4b), the particles were bigger with an X90 above 5 μm, irrespective of the dose and the use of sweeper crystals. Fig. 4c shows the emitted dose for the same conditions with and without sweeper crystals. It is apparent that the sweeper crystals do help dispersion from the inhaler, reflected in a higher emitted dose for both the 30 and 50 mg groups that included sweeper crystals. The most pronounced effect was observed for the 50 mg dose, where sweeper crystals led to an average emitted dose of 93%, which was a 40% increase compared to the formulation without sweeper crystals. Fig. 4d shows the FPF of the emitted aerosol after dispersion from the cyclops inhaler. It can be seen that, independently of the loaded dose and the use of sweeper crystals, the FPF of the emitted powder is comparable, confirming the crystals do not play a role in the deagglomeration itself.

3.2.3. Assessing the aerodynamic properties of the powder through cascade impaction

Next, we assessed the aerodynamic properties of the powder by cascade impaction. Fig. 5 shows the deposition of powder on all stages of the impactor relative to the metered dose. The last bar represents the FPF as a fraction of the emitted dose. It can be seen that the inhaler retention is remarkably low, although a considerable amount (~25%) is retained in the induction port. This can likely be explained by the high loaded dose of around 50 mg and corresponds to previous results [29]. The FPF was found to be 43.2% on average. The MMAD of the delivered dose (emitted dose minus retention and induction port deposit) was 3.4 ± 0.28 μm. The large difference between the FPF found in this measurement and the FPF as determined by laser diffraction (82%, Fig. 4d) can be explained to a significant extent by the large fraction of powder that remains in the induction port of the NGI. This is likely due to the collision of dispersed powder particles to the walls of the induction port which, in the laser diffraction analysis, may have partially added up to the FPF.

3.3. In vitro dose-response assays in Vero-cells

To validate if CD-MUS retained its antiviral activity upon spray drying, an in vitro dose-response assay was performed on both RSV-A (Fig. 6a) and RSV-B (Fig. 6b) in Vero-cells. Virus-compound mixtures were added to cells after pre-incubation of the viruses with either the spray-dried CD-MUS formulation, freeze-dried CD-MUS (stock) or the spray-dried β-CD formulation as a control. From the graphs, it can be seen that CD-MUS, spray-dried together with 4% trileucine, was equally effective as the unformulated compound against both RSV-A (Fig. 6a) and RSV-B (Fig. 6b). This is also confirmed by the comparable IC50 values: 35.2 μg/mL for the stock against RSV-A versus 36.1 μg/mL μg/mL for the dried formulation, and 65.4 μg/mL for the stock against RSV-B versus 43.75 μg/mL for the dried formulation. The lower IC50 against RSV-B resulting from the powder formulation compared to the stock can likely be attributed to individual outliers. As expected, β-CD spray-dried together with 4% trileucine did not elicit any activity against RSV-A nor against RSV-B.

4. Discussion

The possibility to treat respiratory virus infections, like RSV, at their port of entry, i.e. the respiratory tract would be of great interest. This approach ensures rapid acting of the drug without the need to reach the plasma levels required to get adequate concentrations in the lung, which is the case when administered parenterally or orally. In this light, inhalation is obviously the most efficient way to reach high drug concentrations at the site of action without adverse events originating from high plasma concentrations [34].

In the present study, we aimed to develop an inhalable powder formulation of CD-MUS, a novel HSPG-mimicking entry inhibitor. To this end, we first performed a pharmacokinetic and safety assessment to ensure that the compound can safely be administered to the respiratory tract, and, to obtain information of the local and systemic concentrations achieved after administration to the respiratory tract. Our results show that CD-MUS has favorable pharmacokinetic properties after intranasal/pulmonary administration to mice. It can be argued that for envisioning pulmonary administration of the drug as a powder, a pharmacokinetic profile should also be based on pulmonary administration of the drug as a powder. However, in contrast to humans, accurate dosing of powders to the whole respiratory tract of laboratory animals, such as mice, is

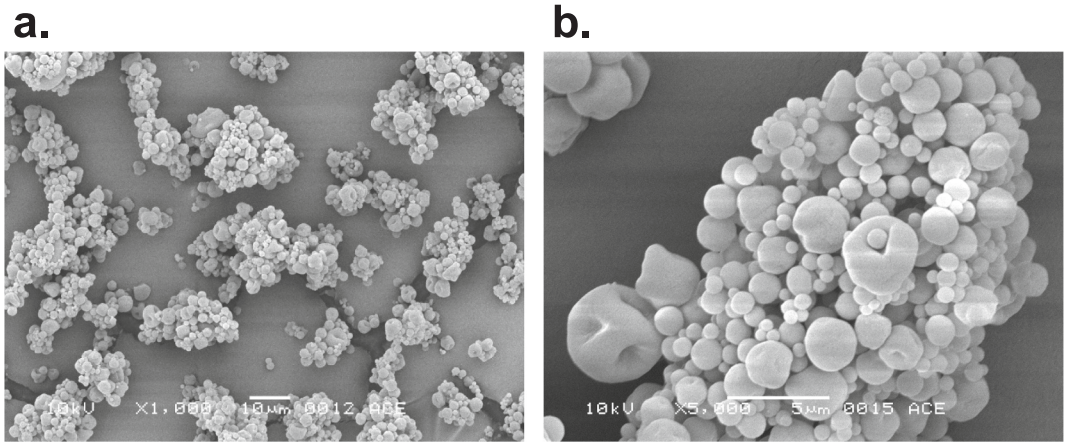

Fig. 3. SEM images of CD-MUS 4% *w*/w trileucine after spray drying. A) macro-view of the powder at a 1000× magnification. Scale bar is 10 μm. B) the same powder shown at 5000× magnification. Scale bar is 5 μm.

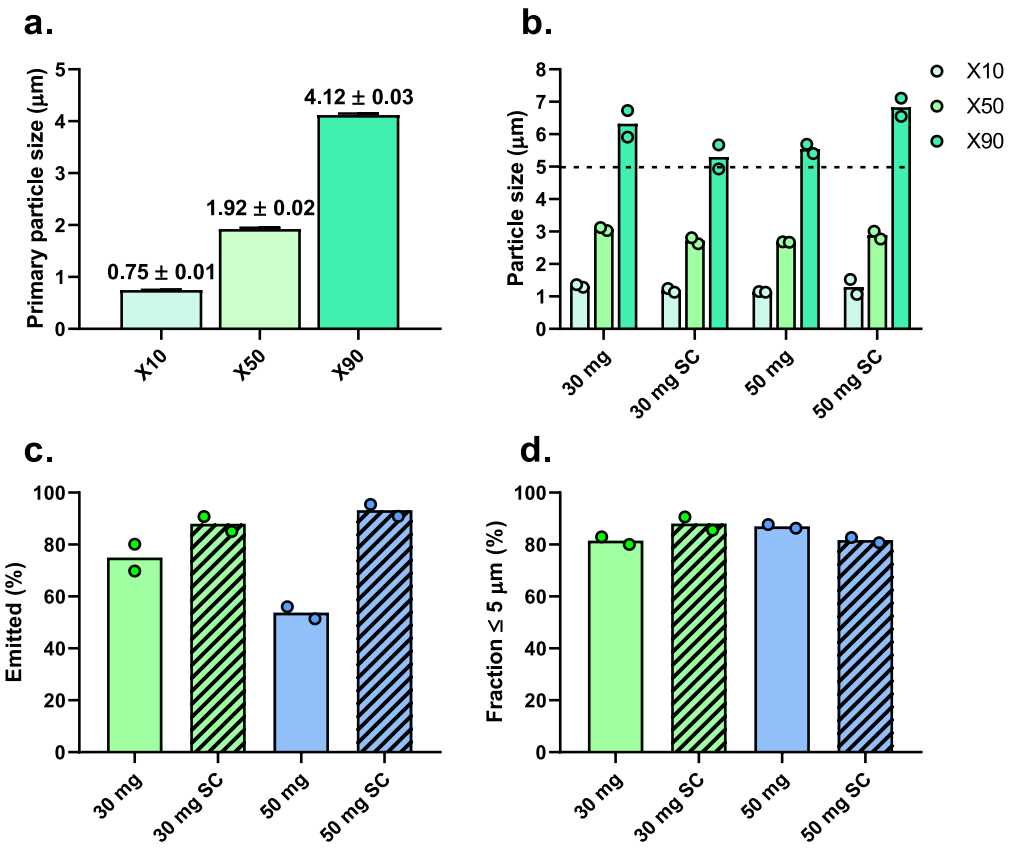

Fig. 4. Particle size analysis and dispersion efficiency of CD-MUS 4% trileucine. A) Particle size distributions after dispersion by the RODOS disperser (primary particles), represented by X10, X50 and X90 values. B) Particle size distributions after dispersion by the Cyclops DPI for four conditions: 30 mg metered dose, 30 mg with sweeper crystals, 50 mg, and 50 mg with sweeper crystals. C) Emitted dose as a percentage of the metered dose for all four conditions. D) The fine particle fraction ≤5 µm as a measure of dispersion efficiency for all conditions. Primary particle size measurements were performed in triplicate. Inhaler measurements were performed in duplicate. Error bars in A represent the standard error of the mean. Dashed line in B represents 5 µm. Abbreviation: SC: sweeper crystals.

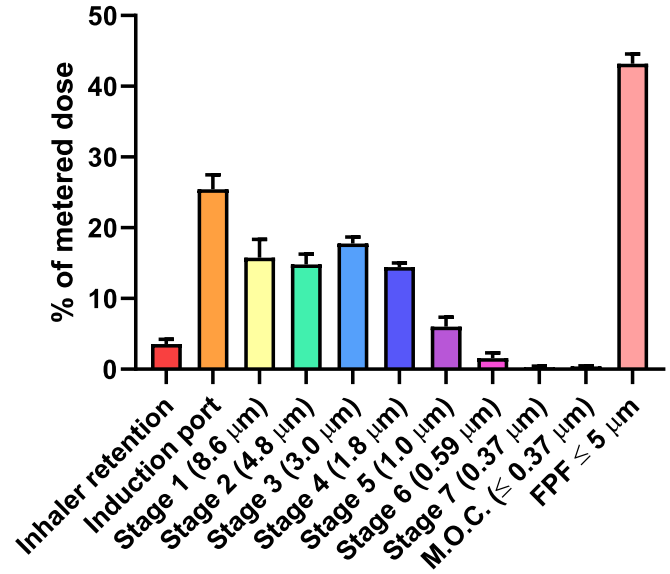

Fig. 5. Relative deposition of CD-MUS 4% trileucine on the impactor stages after dispersion from the cyclops inhaler at 4 kPa pressure drop. Data represent the average deposition on each of the impactor stages as a percentage of the metered dose. The stage-specific cut-off diameters are shown in the x-axis titles. In addition, the retention in the inhaler and induction port is shown as well as the fine particle fraction. Abbreviation: M.O.C.: micro-orifice collector. $n = 4$. Error bars indicate the standard error of the mean.

complicated as inhalers developed for humans can obviously not be used. Moreover, as the mice were anesthetized preceding the treatment, a substantial amount of the liquid is distributed to the lungs anyway. This effect has been observed previously after intranasal instillation of anesthetized mice with volumes as little as 10 µL [22]. Therefore, intranasal instillation is often used in mice to mimic the pharmacokinetic properties for drugs where inhalation is the envisioned administration route. Indeed, CD-MUS was detectable at high concentrations in the lungs already 15 min post-administration with a mean residence time of 90 min, Therefore the intranasal administration can be considered as a combined intranasal/pulmonary administration. Furthermore, our study shows that CD-MUS was adsorbed from the pulmonary tract, confirming a systemic exposure.

Based on these results, CD-MUS was formulated into an inhalable powder using spray drying. In order to increase its dispersion behavior, trileucine was included in the formulation as a dispersion enhancer. Currently, the use of trileucine as an excipient for inhalation has not yet been approved. However, as it is composed of three repeats of L-Leucine, which has been found to be well-tolerated, no notable toxicity is expected [35]. In addition, although no long-term stability tests have been performed in the present study, it is likely that the hydrophobic nature of the surface-active excipient trileucine aids in moisture protection of the spray-dried powder [24]. The particles in the powder were found to be uniform in size as shown by SEM and primary particle size measurements. In addition, they dispersed well from the Cyclops DPI with an emitted dose surpassing 90% and an FPF of 82%. Supporting these results, cascade impaction analysis showed a favorable aerodynamic profile of the powder, reflected in both the FPF (43%) and MMAD (3.4 µm) values. While in the current study, we only assessed the powder's aerodynamic properties at a 4 kPa pressure drop, further studies could test the dispersibility of CD-MUS across a range of pressure drops in order to assess potential deviations in aerosol performance through the impactor [36].

Next, we investigated whether dried CD-MUS retained its activity against RSV. Using an in vitro dose-response assay, we confirmed that the spray-dried compound retained its activity against both RSV-A and RSV-B. This implies that the drying procedure does not affect the

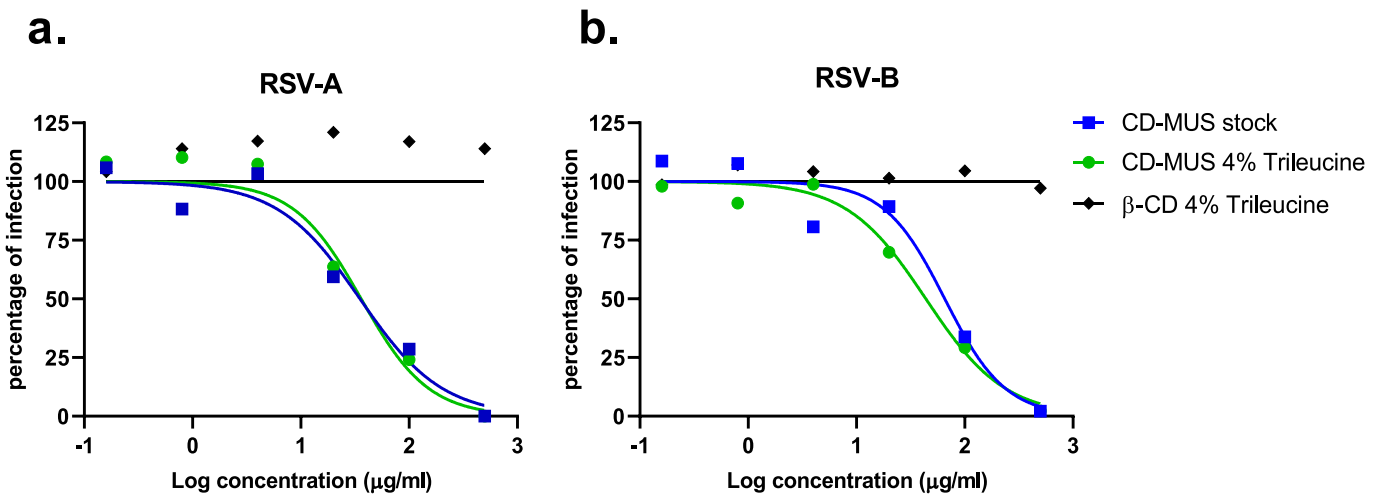

Fig. 6. Dose-response curves were made after co-treatment of Vero-cells with pre-incubated antiviral-virus mixtures. Graphs represent the percentage of infection after treatment with several dilutions of CD-MUS stock solution, CD-MUS spray-dried with 4% trileucine and β-CD spray-dried with 4% trileucine while maintaining a fixed amount of virus (MOI 1). A) RSV-A; B) RSV-B. Percentages are expressed as relative to the untreated control which was set to 100%.

binding of the drug and thus, does not impair its virucidal activity. Given this result, it is to be expected that CD-MUS in its dried form will also be efficacious against previously validated targets, such as herpes simplex virus, dengue virus, and Zika virus, although other transmission routes do not necessitate administration via the respiratory tract.

The relatively high IC_{50} values reported here (35.2 µg/mL of the unformulated compound against RSV-A and 65.21 µg/mL against RSV-B) compared to the IC_{50} values reported previously by Jones et al. (9.11 µg/mL against RSV-A and 5.48 µg/mL against RSV-B) are likely the result of the hundred-fold higher amount of virus used in the present study (MOI 1 compared to MOI 0.01) [19]. As for RSV-A the average percentage of infection in the untreated cells was 54% and for RSV-B 36%, more of the compound is needed to achieve the same degree of inhibition. Another reason could be a difference in the particle to plaque forming unit (PFU) ratio, thus, the ratio of total viral particles to infectious viral particles. This ratio can vary a lot between different viruses (e.g. RSV-A and RSV-B) and different virus batches [37]. In addition, some differences may have arisen from the cell lines used for virus propagation. Specifically, Jones et al. used HEp-2 cells to cultivate their virus while here, the virus was propagated in Vero-cells [19]. It has been reported that RSV virions propagated on Vero-cells contain a cleaved form of the RSV G-protein (i.e. the attachment protein) that leads to altered receptor specificity and makes them five times less infectious to primary human bronchial epithelial cultures (HBE) [38]. This might also have affected their binding affinity for HSPGs and thus for CD-MUS.

In relation to this, there has been a debate as a whole on the dependency of (circulating) RSV for HSPGs as attachment receptor [18,39]. Interestingly, Johnson et al. showed that HSPG is not present on the apical side of HBE cultures while, nevertheless, they are permissive to RSV infection [40]. A range of studies have shown that RSV rather relies on attachment to the CX3C receptor-1 on ciliated cells [40–43]. Research that has studied the interaction of RSV with its host environment has often used laboratory-adapted strains of RSV that were propagated in immortalized cell lines, such as the HEp-2 cell line or, in our case, Vero-cells. In a seminal study by King and colleagues [44], it was found that clinical strains of RSV and strains that were propagated in primary human bronchial epithelial (HBE) cultures had lower affinity for HSPGs than the laboratory-adapted strains. The reason proposed for this diminished affinity is a post-translational modification that leads to a larger (170 kDa) version of the G-protein used for attachment of RSV virions to the host cell [38,44]. In turn, this presumably leads to a partial blockage of the heparin binding pocket [44]. The authors therefore conclude that, for studying virus-host interactions, it would be of high relevance to use strains that are propagated in their host environment [44]. Although they do not affect the results presented here, these findings may be of relevance when considering further exploration of CD-MUS in the (pre-)clinical stages of development. Specifically, they urge the need for validating its efficacy against a broader range of potentially HSPG-independent RSV strains that have either been isolated from patients or have originated from cultures that are more reflective of the host environment.

Delivery of CD-MUS via inhalation using DPIs would primarily be interesting for treatment of the elderly population and other immunocompromised individuals. The use of DPIs in young children, the other patient group prone to severe RSV infections, is precluded because newborns are obligate nose breathers and even toddlers are not able to perform an adequate inhalation maneuver. [45]. In addition, taking into account the child's airway geometry, devices specific to the pediatric population would be needed [46]. Recently, a thorough and promising overview of DPI developments and case studies specific to the pediatric patient group has been presented by Bass and coworkers [47]. In this review, several options are considered, even for the infant population, such as devices for positive-pressure nose-to-lung delivery.

In conclusion, we show that CD-MUS, a novel HSPG-mimicking entry inhibitor is well tolerated after respiratory tract administration in vivo. Using spray drying, an inhalable powder was obtained that disperses well from a DPI and retains its activity against both RSV-A and RSV-B upon drying. Based on the results presented here, future studies should assess the efficacy of pulmonary administered CD-MUS in an in vivo RSV-infection model. Specifically, pulmonary administration should be compared head-to-head with intranasal administration to define any superior effects of one route of administration over the other.

Funding

This research was funded by Schweizerischer Nationalfonds zur Förderung der Wissenschaftlichen Forschung, grant number CRSII5_180323 to F.S. and H.W.F., and by the Dutch Ministry of Health, Welfare and Sports as a funder for A.J.L. and P.B.V.K.

CRediT authorship contribution statement

Rick Heida: Conceptualization, Formal analysis, Investigation, Writing – original draft, Writing – review & editing, Visualization. **Renate Akkerman:** Conceptualization, Formal analysis, Investigation, Writing – original draft, Visualization. **Paulo H. Jacob Silva:** Formal

analysis, Investigation, Writing – original draft, Visualization. **Anke J. Lakerveld:** Investigation, Writing – original draft. **Daniel Ortiz:** Formal analysis, Investigation. **Chiara Bigogno:** Formal analysis, Investigation. **Matteo Gasbarri:** Investigation, Writing – original draft. **Puck B. van Kasteren:** Writing – review & editing, Supervision, Resources. **Francesco Stellacci:** Writing – review & editing, Supervision, Resources, Funding acquisition. **Henderik W. Frijlink:** Conceptualization, Writing – review & editing, Supervision, Resources, Funding acquisition. **Anke L.W. Huckriede:** Conceptualization, Writing – review & editing, Supervision, Resources. **Wouter L.J. Hinrichs:** Conceptualization, Writing – review & editing, Supervision.

Declaration of Competing Interest

Francesco Stellacci is inventor on patent number WO 2018/015465 A1 - Virucidal compounds and uses thereof. Francesco Stellacci and Paulo H. Jacob Silva are co-founders of Asterivir, a start-up company that focuses on developing novel antivirals. The employer of Henderik W. Frijlink holds a license agreement with PureIMS on the Twincer and Cyclops dry powder inhalers. The funders had no role in the design of the study; in the collection, analyses, or interpretation of data; nor in the writing of the manuscript or in the decision to submit the article for publication.

Data availability

Data will be made available on request.

Acknowledgments

The authors thank Doetie Gjaltema (University of Groningen) for assisting with the cascade impaction experiments.

Appendix A. Supplementary data

Supplementary data to this article can be found online at https://doi.org/10.1016/j.jconrel.2023.03.059.

References

[1] J. Piret, G. Boivin, Pandemics throughout history, Front. Microbiol. 11 (2021), 631736, https://doi.org/10.3389/fmicb.2020.631736.

[2] X. Jin, J. Ren, R. Li, Y. Gao, H. Zhang, J. Li, J. Zhang, X. Wang, G. Wang, Global burden of upper respiratory infections in 204 countries and territories, from 1990 to 2019, EClinicalMedicine. 37 (2021), 100986, https://doi.org/10.1016/j.eclinm.2021.100986.

[3] H.H. Kyu, A. Vongpradith, S.B. Sirota, A. Novotney, C.E. Troeger, M.C. Doxey, R. G. Bender, J.R. Ledesma, M.H. Biehl, S.B. Albertson, J.J. Frostad, K. Burkart, F. B. Bennitt, J.T. Zhao, W.M. Gardner, H. Hagins, D. Bryazka, R.-M.V. Dominguez, S. M. Abate, M. Abdelmasseh, A. Abdoli, G. Abdoli, A. Abedi, V. Abedi, T.M. Abegaz, H. Abidi, R.G. Aboagye, H. Abolhassani, Y.D. Abtew, H. Abubaker Ali, E. Abu-Gharbieh, A. Abu-Zaid, K. Adamu, I.Y. Addo, O.A. Adegboye, M. Adnan, Q.E. S. Adnani, M.S. Afzal, S. Afzal, B.O. Ahinkorah, A. Ahmad, A.R. Ahmad, S. Ahmad, A. Ahmadi, S. Ahmadi, H. Ahmed, J.Q. Ahmed, T. Ahmed Rashid, M. Akbarzadeh-Khiavi, H. Al Hamad, L. Albano, M.A. Aldeyab, B.M. Alemu, K.A. Alene, A. M. Algammal, F.A.N. Alhalaiqa, R.K. Alhassan, B.A. Ali, L. Ali, M.M. Ali, S.S. Ali, Y. Alimohamadi, V. Alipour, A. Al-Jumaily, S.M. Aljunid, S. Almustanyir, R.M. Al-Raddadi, R.H.H. Al-Rifai, S.A.S. AlRyalat, N. Alvis-Guzman, N.J. Alvis-Zakzuk, E. K. Ameyaw, J.J. Aminian Dehkordi, J.H. Amuasi, D.A. Amugsi, E.W. Anbesu, A. Ansar, A.E. Anyasodor, J. Arabloo, D. Areda, A.M. Argaw, Z.G. Argaw, J. Arulappan, R.T. Aruleba, M.A. Asemahagn, S.S. Athari, D. Atlaw, E.F. Attia, S. Attia, A. Aujayeb, T. Awoke, T.M. Ayana, M.A. Ayanore, S. Azadnajafabad, M. Azangou-Khyavy, S. Azari, A. Azari Jafari, M. Badar, A.D. Badiye, N. Baghcheghi, S. Bagherieh, A.A. Baig, M. Banach, I. Banerjee, M. Bardhan, F. Barone-Adesi, H.J. Barqawi, A. Barrow, A. Bashiri, Q. Bassat, A.-M.M. Batiha, A. B. Belachew, M.A. Belete, U.I. Belgaumi, A.S. Bhagavathula, N. Bhardwaj, P. Bhardwaj, P. Bhatt, V.S. Bhojaraja, Z.A. Bhutta, S.S. Bhuyan, A. Bijani, S. Bitaraf, B.B.A. Bodicha, N.I. Briko, D. Buonsenso, M.H. Butt, J. Cai, P. Camargos, L. A. Cámera, P.A. Chakraborty, M.G. Chanie, J. Charan, V.K. Chattu, P.R. Ching, S. Choi, Y.Y. Chong, S.G. Choudhari, E.K. Chowdhury, D.J. Christopher, D.-T. Chu, N.L. Cobb, A.J. Cohen, N. Cruz-Martins, O. Dadras, F.T. Dagnaw, X. Dai, L. Dandona, R. Dandona, A.T.M. Dao, S.A. Debela, B. Demisse, F.W. Demisse, S. Demissie, D. Dereje, H.D. Desai, A.A. Desta, B. Desye, S. Dhingra, N. Diao, D. Diaz, L.E. Digesa, L.P. Doan, M. Dodangeh, D. Dongarwar, F. Dorostkar, W. M. dos Santos, H.L. Dsouza, E. Dubljanin, O.C. Durojaiye, H.A. Edinur, E. Ehsani-Chimeh, E. Eini, M. Ekholuenetale, T.C. Ekundayo, E.D. El Desouky, I. El Sayed, M. El Sayed Zaki, M. Elhadi, A.M.R. Elkhapery, A. Emami, L. Engelbert Bain, R. Erkhembayar, F. Etaee, M. Ezati Asar, A.F. Fagbamigbe, S. Falahi, A. Fallahzadeh, A. Faraj, E.J.A. Faraon, A. Fatehizadeh, P. Ferrara, A.A. Ferrari, G. Fetensa, F. Fischer, J. Flavel, M. Foroutan, P.A. Gaal, A.M. Gaidhane, S. Gaihre, N. Galehdar, A.L. Garcia-Basteiro, T. Garg, M.D. Gebrehiwot, M.A. Gebremichael, Y.Y. Gela, B.N.B. Gemeda, B.D. Gessner, M. Getachew, A. Getie, S.-H. Ghamari, M. Ghasemi Nour, A. Ghashghaee, A. Gholamrezanezhad, A. Gholizadeh, R. Ghosh, S. Ghozy, P. Goleij, M. Golitaleb, G. Gorini, A.C. Goulart, G.G. Goyomsa, H. A. Guadie, Z. Gudisa, R.A. Guled, S. Gupta, V.B. Gupta, V.K. Gupta, A. Guta, P. Habibzadeh, A. Haj-Mirzaian, R. Halwani, S. Hamidi, M.A. Hannan, M. Harorani, A.I. Hasaballah, H. Hasani, A.M. Hassan, S. Hassani, H. Hassanian-Moghaddam, H. Hassankhani, K. Hayat, B. Heibati, M. Heidari, D.Z. Heyi, K. Hezam, R. Holla, S.H. Hong, N. Horita, M.-S. Hosseini, M. Hosseinzadeh, M. Hostiuc, M. Househ, S. Hoveidamanesh, J. Huang, N.R. Hussein, I. Iavicoli, S. E. Ibitoye, K.S. Ikuta, O.S. Ilesanmi, I.M. Ilic, M.D. Ilic, M. Immurana, N.E. Ismail, M. Iwagami, J. Jaafari, E. Jamshidi, S.-I. Jang, A. Javadi Mamaghani, T. Javaheri, F. Javanmardi, J. Javidnia, S.K. Jayapal, U. Jayarajah, S. Jayaram, A.T. Jema, W. Jeong, J.B. Jonas, N. Joseph, F. Joukar, J.J. Jozwiak, V.K.Z. Kabir, S.E. O. Kacimi, V. Kadashetti, L.R. Kalankesh, R. Kalhor, A. Kamath, B.D. Kamble, H. Kandel, T.K. Kanko, I.M. Karaye, A. Karch, S. Karkhah, B.G. Kassa, P.D. Katoto, H. Kaur, R.J. Kaur, L. Keikavoosi-Arani, M. Keykhaei, Y.S. Khader, H. Khajuria, E. A. Khan, G. Khan, I.A. Khan, M. Khan, M.N. Khan, M.A. Khan, Y.H. Khan, M. M. Khatatbeh, M. Khosravifar, J. Khubchandani, M.S. Kim, R.W. Kimokoti, A. Kisa, S. Kisa, N. Kissoon, L.D. Knibbs, S. Kochhar, F. Kompani, H.R. Koohestani, V. A. Korshunov, S. Kosen, P.A. Koul, A. Koyanagi, K. Krishan, B. Kuate Defo, G. A. Kumar, O.P. Kurmi, A. Kuttikkattu, D.K. Lal, J. Lám, I. Landires, C. Ledda, S. Lee, M. Levi, S. Lewycka, G. Liu, W. Liu, R. Lodha, L. Lorenzovici, M. Lotfi, J. A. Loureiro, F. Madadizadeh, A. Mahmoodpoor, R. Mahmoudi, M. Mahmoudimanesh, J. Majidpoor, A. Makki, E. Malakan Rad, A.A. Malik, T. H. Mallhi, Y. Manla, C.N. Matei, A.G. Mathioudakis, R.J. Maude, E. Mehrabi Nasab, A. Melese, Z.A. Memish, O. Mendoza-Cano, A.-F.A. Mentis, T.J. Meretoja, M. W. Merid, T. Mestrovic, A.C. Micheletti Gomide Nogueira de Sá, G.F.W. Mijena, L. H.N. Minh, S.A. Mir, R. Mirfakhraie, S. Mirmoeeni, A.Z. Mirza, M. Mirza, M. Mirza-Aghazadeh-Attari, A.S. Misganaw, A.T. Misganaw, E. Mohammadi, M. Mohammadi, A. Mohammed, S. Mohammed, S. Mohan, M. Mohseni, N. Moka, A.H. Mokdad, S. Momtazmanesh, L. Monasta, M. Moniruzzaman, F. Montazeri, C. E. Moore, A. Moradi, L. Morawska, J.F. Mosser, E. Mostafavi, M. Motaghinejad, H. Mousavi Isfahani, S.A. Mousavi-Aghdas, S. Mubarik, E. Murillo-Zamora, G. Mustafa, S. Nair, T.S. Nair, H. Najafi, A.A. Naqvi, S. Narasimha Swamy, Z. S. Natto, B.P. Nayak, S.A. Nejadghaderi, H.V.N. Nguyen, R.K. Niazi, A.T. Nogueira de Sá, H. Nouraei, A. Nowroozi, V. Nuñez-Samudio, C.I. Nzoputam, O. J. Nzoputam, B. Oancea, C. Ochir, O.O. Odukoya, H. Okati-Aliabad, A.P. Okekunle, O.C. Okonji, A.T. Olagunju, I.I. Olufadewa, A. Omar Bali, E. Omer, E. Oren, E. Ota, N. Otstavnov, A. Oulhaj, J.R. Padubidri, K. Pakshir, R. Pakzad, T. Palicz, A. Pandey, S. Pant, S. Pardhan, E.-C. Park, E.-K. Park, F. Pashazadeh Kan, R. Paudel, S. Pawar, M. Peng, G. Pereira, S. Perna, N. Perumalsamy, I.-R. Petcu, D.M. Pigott, Z. Z. Piracha, V. Podder, R.V. Polibin, M.J. Postma, H. Pourasghari, N. Pourtaheri, M. M.F. Qadir, M. Raad, M. Rabiee, N. Rabiee, S. Raeghi, A. Rafiei, F. Rahim, M. Rahimi, V. Rahimi-Movaghar, A. Rahman, M.O. Rahman, M. Rahman, M. A. Rahman, A.M. Rahmani, V. Rahmanian, P. Ram, K. Ramezanzadeh, J. Rana, P. Ranasinghe, U. Rani, S.J. Rao, S. Rashedi, M.-M. Rashidi, A. Rasul, Z.A. Ratan, D. L. Rawaf, S. Rawaf, R. Rawassizadeh, M.S. Razeghinia, E.M.M. Redwan, M. B. Reitsma, A.M.N. Renzaho, M. Rezaeian, A. Riad, R. Rikhtegar, J.A.B. Rodriguez, E.L.B. Rogowski, L. Ronfani, K.E. Rudd, B. Saddik, E. Sadeghi, U. Saeed, A. Safary, S.Z. Safi, M. Sahebazzamani, A. Sahebkar, S. Sakhamuri, S. Salehi, M. Salman, H. Samadi Kafil, A.M. Samy, M.M. Santric-Milicevic, B.P. Sao Jose, M. Sarkhosh, B. Sathian, M. Sawhney, G.K. Saya, A.-A. Seidu, A. Seylani, A.A. Shaheen, M. A. Shaikh, E. Shaker, H. Shamshad, M.M. Sharew, A. Sharhani, A. Sharifi, P. Sharma, A. Sheidaei, S.M. Shenoy, J.K. Shetty, D.S. Shiferaw, M. Shigematsu, J. Il Shin, H. Shirzad-Aski, K.M. Shivakumar, S. Shivalli, P. Shobeiri, W. Simegn, C. R. Simpson, H. Singh, J.A. Singh, P. Singh, S.S. Siwal, V.Y. Skryabin, A. A. Skryabina, M.S. Soltani-Zangbar, S. Song, Y. Song, P. Sood, C.T. Sreeramareddy, P. Steiropoulos, M. Suleman, S.-A. Tabatabaeizadeh, A. Tahamtan, M. Taheri, M. Taheri Soodejani, E. Taki, I.M. Talaat, M. Tampa, S. Tandukar, N.Y. Tat, V.Y. Tat, Y.M. Tefera, G. Temesgen, M.-H. Temsah, A. Tesfaye, D.G. Tesfaye, B. Tessema, R. Thapar, J.H.V. Ticoalu, A. Tiyuri, I.I. Tleyjeh, M. Togtmol, M.R. Tovani-Palone, D.G. Tufa, I. Ullah, E. Upadhyay, S. Valadan Tahbaz, P.R. Valdez, R. Valizadeh, C. Vardavas, T.J. Vasankari, B. Vo, L.G. Vu, B. Wagaye, Y. Waheed, Y. Wang, A. Waris, T.E. West, N.D. Wickramasinghe, X. Xu, S. Yaghoubi, G.A.T. Yahya, S.H. Yahyazadeh Jabbari, D.K. Yon, N. Yonemoto, B.A. Zaman, A. Zandifar, M. Zangiabadian, H.J. Zar, I. Zare, Z. Zareshahrabadi, A. Zarrintan, M. S. Zastrozhin, W. Zeng, M. Zhang, Z.-J. Zhang, C. Zhong, M. Zoladl, A. Zumla, S. S. Lim, T. Vos, M. Naghavi, M. Brauer, S.I. Hay, C.J.L. Murray, Age–sex differences in the global burden of lower respiratory infections and risk factors, 1990–2019: results from the Global Burden of Disease Study 2019, Lancet Infect. Dis. 22 (2022) 1626–1647, https://doi.org/10.1016/S1473-3099(22)00510-2.

[4] Y. Li, X. Wang, D.M. Blau, M.T. Caballero, D.R. Feikin, C.J. Gill, S.A. Madhi, S. B. Omer, E.A.F. Simões, H. Campbell, A.B. Pariente, D. Bardach, Q. Bassat, J.-S. Casalegno, G. Chakhunashvili, N. Crawford, D. Danilenko, L.A.H. Do, M. Echavarria, A. Gentile, A. Gordon, T. Heikkinen, Q.S. Huang, S. Jullien, A. Krishnan, E.L. Lopez, J. Markić, A. Mira-Iglesias, H.C. Moore, J. Moyes, L. Mwananyanda, D.J. Nokes, F. Noordeen, E. Obodai, N. Palani, C. Romero, V. Salimi, A. Satav, E. Seo, Z. Shchomak, R. Singleton, K. Stolyarov, S.K. Stoszek, A. von Gottberg, D. Wurzel, L.-M. Yoshida, C.F. Yung, H.J. Zar, H. Nair, M. Abram,

J. Aerssens, A. Alafaci, A. Balmaseda, T. Bandeira, I. Barr, E. Batinović, P. Beutels, J. Bhiman, C.C. Blyth, L. Bont, S.S. Bressler, C. Cohen, R. Cohen, A.-M. Costa, R. Crow, A. Daley, D.-A. Dang, C. Demont, C. Desnoyers, J. Díez-Domingo, M. Divarathna, M. du Plessis, M. Edgoose, F.M. Ferolla, T.K. Fischer, A. Gebremedhin, C. Giaquinto, Y. Gillet, R. Hernandez, C. Horvat, E. Javouhey, I. Karseladze, J. Kubale, R. Kumar, B. Lina, F. Lucion, R. MacGinty, F. Martinon-Torres, A. McMinn, A. Meijer, P. Milić, A. Morel, K. Mulholland, T. Mungun, N. Murunga, C. Newbern, M.P. Nicol, J.K. Odoom, P. Openshaw, D. Ploin, F. P. Polack, A.J. Pollard, N. Prasad, J. Puig-Barberà, J. Reiche, N. Reyes, B. Rizkalla, S. Satao, T. Shi, S. Sistla, M. Snape, Y. Song, G. Soto, F. Tavakoli, M. Toizumi, N. Tsedenbal, M. van den Berge, C. Vernhes, C. von Mollendorf, S. Walaza, G. Walker, Global, regional, and national disease burden estimates of acute lower respiratory infections due to respiratory syncytial virus in children younger than 5 years in 2019: a systematic analysis, Lancet 399 (2022) 2047–2064, https://doi.org/10.1016/S0140-6736(22)00478-0.

[5] J.G. Wildenbeest, M.-N. Billard, R.P. Zuurbier, K. Korsten, A.C. Langedijk, P.M. van de Ven, M.D. Snape, S.B. Drysdale, A.J. Pollard, H. Robinson, T. Heikkinen, S. Cunningham, T. O'Neill, B. Rizkalla, A. Dacosta-Urbieta, F. Martinón-Torres, M. A. van Houten, L.J. Bont, J. Wildenbeest, M.-N. Billard, R. Zuurbier, K. Korsten, M. van Houten, A. Langedijk, P. van de Ven, L. Bont, S. Drysdale, J. McGinley, G.-L. Lin, M. Snape, A. Pollard, A. Ives, H. Wolfenden, S. Salgia, R. Shetty, A. Dacosta-Urbieta, I. Rivero-Calle, A. Gómez-Carballa, S. Pischedda, C. Rodriguez-Tenreiro, F. Martinón-Torres, T. Heikkinen, S. Cunningham, H. Nair, H. Campbell, T. O'Neill, M. Miller, J. Baggott, C. Beveridge, R. McKernan, B. Rizkalla, P. Beutels, P. Openshaw, A. Meijer, T. Kølsen Fischer, M. van den Berge, C. Giaquinto, M. Abram, K. Swanson, J. Aerssens, C. Vernhes, S. Gallichan, V. Kumar, E. Molero, The burden of respiratory syncytial virus in healthy term-born infants in Europe: a prospective birth cohort study, Lancet Respir. Med. 0 (2022), https://doi.org/10.1016/S2213-2600(22)00414-3.

[6] B. Ackerson, H.F. Tseng, L.S. Sy, Z. Solano, J. Slezak, Y. Luo, C.A. Fischetti, V. Shinde, Severe morbidity and mortality associated with respiratory syncytial virus versus influenza infection in hospitalized older adults, Clin. Infect. Dis. 69 (2019) 197–203, https://doi.org/10.1093/cid/ciy991.

[7] C.K. Johnson. What is RSV and why is it surging across the U.S.?, PBS NewsHour, 2022. https://www.pbs.org/newshour/health/what-is-rsv-and-why-is-it-surging-across-the-u-s (accessed October 26, 2022).

[8] K. Messacar, R.E. Baker, S.W. Park, H. Nguyen-Tran, J.R. Cataldi, B. Grenfell, Preparing for uncertainty: endemic paediatric viral illnesses after COVID-19 pandemic disruption, Lancet. 0 (2022), https://doi.org/10.1016/S0140-6736(22)01277-6.

[9] A.J. Pollard, E.M. Bijker, A guide to vaccinology: from basic principles to new developments, Nat. Rev. Immunol. 21 (2021) 83–100, https://doi.org/10.1038/s41577-020-00479-7.

[10] A.E.S. de Zwart, A. Riezebos-Brilman, H.A.M. Kerstjens, E.A.M. Verschuuren, J.-W. C. Alffenaar, Respiratory syncytial virus infection morbidity in the elderly: time for repurposing of ribavirin? Clin. Infect. Dis. 70 (2020) 2238–2239, https://doi.org/10.1093/cid/ciz835.

[11] M.S. Luna, P. Manzoni, B. Paes, E. Baraldi, V. Cossey, A. Kugelman, R. Chawla, A. Dotta, R. Rodríguez Fernández, B. Resch, X. Carbonell-Estrany, Expert consensus on palivizumab use for respiratory syncytial virus in developed countries, Paediatr. Respir. Rev. 33 (2020) 35–44, https://doi.org/10.1016/j.prrv.2018.12.001.

[12] L.L. Hammitt, R. Dagan, Y. Yuan, M. Baca Cots, M. Bosheva, S.A. Madhi, W. J. Muller, H.J. Zar, D. Brooks, A. Grenham, U. Wählby Hamrén, V.S. Mankad, P. Ren, T. Takas, M.E. Abram, A. Leach, M.P. Griffin, T. Villafana, Nirsevimab for prevention of RSV in healthy late-preterm and term infants, N. Engl. J. Med. 386 (2022) 837–846, https://doi.org/10.1056/NEJMoa2110275.

[13] M. Beugeling, J. De Zee, H.J. Woerdenbag, H.W. Frijlink, J.C. Wilschut, W.L. J. Hinrichs, Respiratory syncytial virus subunit vaccines based on the viral envelope glycoproteins intended for pregnant women and the elderly, Expert Rev. Vaccines. 18 (2019) 935–950, https://doi.org/10.1080/14760584.2019.1657013.

[14] A. Pelaez, G.M. Lyon, S.D. Force, A.M. Ramirez, D.C. Neujahr, M. Foster, P.M. Naik, A.A. Gal, P.O. Mitchell, E.C. Lawrence, Efficacy of oral ribavirin in lung transplant patients with respiratory syncytial virus lower respiratory tract infection, J. Hear. Lung Transplant. 28 (2009) 67–71, https://doi.org/10.1016/j.healun.2008.10.008.

[15] R. Heida, Y.C. Bhide, M. Gasbarri, Ö. Kocabiyik, F. Stellacci, A.L.W. Huckriede, W. L.J. Hinrichs, H.W. Frijlink, Advances in the development of entry inhibitors for sialic-acid-targeting viruses, Drug Discov. Today 26 (2021) 122–137, https://doi.org/10.1016/j.drudis.2020.10.009.

[16] O. Kocabiyik, V. Cagno, P.J. Silva, Y. Zhu, L. Sedano, Y. Bhide, J. Mettier, C. Medaglia, B. Da Costa, S. Constant, S. Huang, L. Kaiser, W.L.J. Hinrichs, A. Huckriede, R. Le Goffic, C. Tapparel, F. Stellacci, Non-toxic virucidal macromolecules show high efficacy against influenza virus ex vivo and in vivo, Adv. Sci. 8 (2021) 2001012, https://doi.org/10.1002/advs.202001012.

[17] V. Cagno, P. Andreozzi, M. D'Alicarnasso, P. Jacob Silva, M. Mueller, M. Galloux, R. Le Goffic, S.T. Jones, M. Vallino, J. Hodek, J. Weber, S. Sen, E.-R. Janeček, A. Bekdemir, B. Sanavio, C. Martinelli, M. Donalisio, M.-A. Rameix Welti, J.-F. Eleouet, Y. Han, L. Kaiser, L. Vukovic, C. Tapparel, P. Král, S. Krol, D. Lembo, F. Stellacci, Broad-spectrum non-toxic antiviral nanoparticles with a virucidal inhibition mechanism, Nat. Mater. 17 (2018) 195–203, https://doi.org/10.1038/nmat5053.

[18] V. Cagno, E.D. Tseligka, S.T. Jones, C. Tapparel, Heparan sulfate proteoglycans and viral attachment: true receptors or adaptation Bias? Viruses. 11 (2019) 596, https://doi.org/10.3390/v11070596.

[19] S.T. Jones, V. Cagno, M. Janeček, D. Ortiz, N. Gasilova, J. Piret, M. Gasbarri, D. A. Constant, Y. Han, L. Vuković, P. Král, L. Kaiser, S. Huang, S. Constant, K. Kirkegaard, G. Boivin, F. Stellacci, C. Tapparel, Modified cyclodextrins as broad-spectrum antivirals, Sci. Adv. 6 (2020), https://doi.org/10.1126/sciadv.aax9318.

[20] V. Cagno, M. Gasbarri, C. Medaglia, D. Gomes, S. Clement, F. Stellacci, C. Tapparel, Sulfonated nanomaterials with broad-spectrum antiviral activity extending beyond heparan sulfate-dependent viruses, Antimicrob. Agents Chemother. 64 (2020), https://doi.org/10.1128/AAC.02001-20.

[21] L. Zhang, M.E. Peeples, R.C. Boucher, P.L. Collins, R.J. Pickles, Respiratory syncytial virus infection of human airway epithelial cells is polarized, specific to ciliated cells, and without obvious cytopathology, J. Virol. 76 (2002) 5654–5666, https://doi.org/10.1128/JVI.76.11.5654-5666.2002.

[22] D.S. Southam, M. Dolovich, P.M. O'Byrne, M.D. Inman, Distribution of intranasal instillations in mice: effects of volume, time, body position, and anesthesia, Am. J. Physiol. Cell. Mol. Physiol. 282 (2002) L833–L839, https://doi.org/10.1152/ajplung.00173.2001.

[23] I. Sibum, P. Hagedoorn, M.P.G. Kluitman, M. Kloezen, H.W. Frijlink, F. Grasmeijer, Dispersibility and storage stability optimization of high dose isoniazid dry powder inhalation formulations with L-leucine or trileucine, Pharmaceutics. 12 (2019) 24, https://doi.org/10.3390/pharmaceutics12010024.

[24] M. Ordoubadi, F.K.A. Gregson, H. Wang, N.B. Carrigy, M. Nicholas, S. Gracin, D. Lechuga-Ballesteros, J.P. Reid, W.H. Finlay, R. Vehring, Trileucine as a dispersibility enhancer of spray-dried inhalable microparticles, J. Control. Release 336 (2021) 522–536, https://doi.org/10.1016/j.jconrel.2021.06.045.

[25] D. Lechuga-Ballesteros, C. Charan, C.L.M. Stults, C.L. Stevenson, D.P. Miller, R. Vehring, V. Tep, M. Kuo, Trileucine improves aerosol performance and stability of spray-dried powders for inhalation, J. Pharm. Sci. 97 (2008) 287–302, https://doi.org/10.1002/jps.21078.

[26] I. Sibum, P. Hagedoorn, C.O. Botterman, H.W. Frijlink, F. Grasmeijer, Automated filling equipment allows increase in the maximum dose to be filled in the Cyclops® high dose dry powder inhalation device while maintaining dispersibility, Pharmaceutics. 12 (2020) 645, https://doi.org/10.3390/pharmaceutics12070645.

[27] M. Hoppentocht, O.W. Akkerman, P. Hagedoorn, H.W. Frijlink, A.H. de Boer, The Cyclops for pulmonary delivery of aminoglycosides; a new member of the TwincerTM family, Eur. J. Pharm. Biopharm. 90 (2015) 8–15, https://doi.org/10.1016/j.ejpb.2015.01.012.

[28] Directorate for the Quality of Medicines & HealthCare of the Council of Europe (EDQM), Preparations for inhalation: aerodynamic assessment of fine particles, in: Eur. Pharmacopoeia, 9th ed., 2016, pp. 331–335.

[29] F. Grasmeijer, P. Hagedoorn, H.W. Frijlink, A.H. de Boer, Characterisation of high dose aerosols from dry powder inhalers, Int. J. Pharm. 437 (2012) 242–249, https://doi.org/10.1016/j.ijpharm.2012.08.020.

[30] R. Dreywood, Qualitative test for carbohydrate material, Ind. Eng. Chem. Anal. Ed. 18 (1946) 499, https://doi.org/10.1021/i560156a015.

[31] M. Luinstra, F. Grasmeijer, P. Hagedoorn, J.R. Moes, H.W. Frijlink, A.H. de Boer, A levodopa dry powder inhaler for the treatment of Parkinson's disease patients in off periods, Eur. J. Pharm. Biopharm. 97 (2015) 22–29, https://doi.org/10.1016/j.ejpb.2015.10.003.

[32] Y. van Remmerden, F. Xu, M. van Eldik, J.G.M. Heldens, W. Huisman, M. N. Widjojoatmodjo, An improved respiratory syncytial virus neutralization assay based on the detection of green fluorescent protein expression and automated plaque counting, Virol. J. 9 (2012) 253, https://doi.org/10.1186/1743-422X-9-253.

[33] J.C. Hierholzer, R.A. Killington, Virus isolation and quantitation, in: Virol. Methods Man, Elsevier, 1996, pp. 25–46, https://doi.org/10.1016/B978-012465330-6/50003-8.

[34] M. Hoppentocht, P. Hagedoorn, H.W. Frijlink, A.H. de Boer, Technological and practical challenges of dry powder inhalers and formulations, Adv. Drug Deliv. Rev. 75 (2014) 18–31, https://doi.org/10.1016/j.addr.2014.04.004.

[35] D. Zillen, M. Beugeling, W.L.J. Hinrichs, H.W. Frijlink, F. Grasmeijer, Natural and bioinspired excipients for dry powder inhalation formulations, Curr. Opin. Colloid Interface Sci. 56 (2021), 101497, https://doi.org/10.1016/j.cocis.2021.101497.

[36] J. Rudén, G. Frenning, T. Bramer, K. Thalberg, G. Alderborn, Effect of pressure drop on the in vitro dispersion of adhesive mixtures of different blend states for inhalation, Int. J. Pharm. 617 (2022), 121590, https://doi.org/10.1016/j.ijpharm.2022.121590.

[37] S.M. Perkins, D.L. Webb, S.A. Torrance, C. El Saleeby, L.M. Harrison, J.A. Aitken, A. Patel, J.P. DeVincenzo, Comparison of a real-time reverse transcriptase PCR assay and a culture technique for quantitative assessment of viral load in children naturally infected with respiratory syncytial virus, J. Clin. Microbiol. 43 (2005) 2356–2362, https://doi.org/10.1128/JCM.43.5.2356-2362.2005.

[38] S. Kwilas, R.M. Liesman, L. Zhang, E. Walsh, R.J. Pickles, M.E. Peeples, Respiratory syncytial virus grown in Vero cells contains a truncated attachment protein that alters its infectivity and dependence on Glycosaminoglycans, J. Virol. 83 (2009) 10710–10718, https://doi.org/10.1128/JVI.00986-09.

[39] Z. Feng, L. Xu, Z. Xie, Receptors for respiratory syncytial virus infection and host factors regulating the life cycle of respiratory syncytial virus, Front. Cell. Infect. Microbiol. 12 (2022) 130, https://doi.org/10.3389/fcimb.2022.858629.

[40] S.M. Johnson, B.A. McNally, I. Ioannidis, E. Flano, M.N. Teng, A.G. Oomens, E. E. Walsh, M.E. Peeples, Respiratory syncytial virus uses CX3CR1 as a receptor on primary human airway epithelial cultures, PLoS Pathog. 11 (2015), e1005318, https://doi.org/10.1371/journal.ppat.1005318.

[41] K.-I. Jeong, P.A. Piepenhagen, M. Kishko, J.M. DiNapoli, R.P. Groppo, L. Zhang, J. Almond, H. Kleanthous, S. Delagrave, M. Parrington, CX3CR1 is expressed in differentiated human ciliated airway cells and co-localizes with respiratory syncytial virus on cilia in a G protein-dependent manner, PLoS One 10 (2015), e0130517, https://doi.org/10.1371/journal.pone.0130517.

[42] T. Chirkova, S. Lin, A.G.P. Oomens, K.A. Gaston, S. Boyoglu-Barnum, J. Meng, C. C. Stobart, C.U. Cotton, T.V. Hartert, M.L. Moore, A.G. Ziady, L.J. Anderson, CX3CR1 is an important surface molecule for respiratory syncytial virus infection in human airway epithelial cells, J. Gen. Virol. 96 (2015) 2543–2556, https://doi.org/10.1099/vir.0.000218.

[43] C.S. Anderson, C.-Y. Chu, Q. Wang, J.A. Mereness, Y. Ren, K. Donlon, S. Bhattacharya, R.S. Misra, E.E. Walsh, G.S. Pryhuber, T.J. Mariani, CX3CR1 as a respiratory syncytial virus receptor in pediatric human lung, Pediatr. Res. 87 (2020) 862–867, https://doi.org/10.1038/s41390-019-0677-0.

[44] T. King, A. Mejias, O. Ramilo, M.E. Peeples, The larger attachment glycoprotein of respiratory syncytial virus produced in primary human bronchial epithelial cultures reduces infectivity for cell lines, PLoS Pathog. 17 (2021), e1009469, https://doi.org/10.1371/journal.ppat.1009469.

[45] D.N. Price, N.K. Kunda, P. Muttil, Challenges associated with the pulmonary delivery of therapeutic dry powders for preclinical testing, KONA Powder Part. J. 36 (2019) 129–144, https://doi.org/10.14356/kona.2019008.

[46] A.J. Lexmond, P. Hagedoorn, H.W. Frijlink, B.L. Rottier, A.H. de Boer, Prerequisites for a dry powder inhaler for children with cystic fibrosis, PLoS One 12 (2017), e0183130, https://doi.org/10.1371/journal.pone.0183130.

[47] K. Bass, D. Farkas, A. Hassan, S. Bonasera, M. Hindle, P.W. Longest, High-efficiency dry powder aerosol delivery to children: review and application of new technologies, J. Aerosol Sci. 153 (2021), 105692, https://doi.org/10.1016/j.jaerosci.2020.105692.